Research article

Synergistic effects between acidity and the crystalline phases of thermally activated layered Zn hydroxide nitrate on the methanolysis of acidic soybean oils

Siwaporn Meejoo Smith [a], Wilasinee Lerdrittipong [a,b], Warisara Woranuch [a], Suwilai Chaveanghong [a,c], Shangeetha Ganesan [d,*]

[a] Center of Sustainable Energy and Green Materials, and Department of Chemistry, Faculty of Science, Mahidol University, 999 Phuttamonthon Sai 4 Rd., Salaya, Nakhon Pathom, 73170, Thailand
[b] Center of Excellence for Innovation in Chemistry, 272 Thanon Rama VI, Thung Phaya Thai, Ratchathewi, Bangkok, 10400, Thailand
[c] Mahidol University Frontier Research Facility, Mahidol University, 999 Phuttamonthon Sai 4 Rd., Salaya, Nakhon Pathom, 73170, Thailand
[d] School of Chemical Sciences, Universiti Sains Malaysia, 11800, USM, Penang, Malaysia

ARTICLE INFO

ABSTRACT

Layered hydroxyl salts (LHS) is a promising catalyst in the field of methanolysis (transesterification and esterification reactions) of oil feedstocks. The catalytic activity of the catalyst can be enhanced with heat treatment. The present study investigated the relationship between thermal stability of the layered Zn hydroxide nitrate (ZHN), their acid-base properties, and the catalytic conversion of oil feedstocks to methyl ester. The solid, predominantly acidic catalyst was prepared at various temperatures (70–170 °C) and tested for the acidic/basic properties using the Hammett indicators and titration method followed by functional group analysis using FTIR, crystallization using X-ray diffraction, and surface morphology using SEM. The combination of various characterization techniques gave an insight into the changes in the phases of the layered Zn hydroxide nitrate catalysts upon thermal treatment. Major phase changes occurred at temperatures somewhat above 80, and 140 °C. The catalysts were extensively studied to understand the underlying effects on the FAME yields obtained from catalytic conversion of oleic acid spiked soy bean oil (a model of an acidic oil feedstock) into methyl esters. The results of the optimization reactions reaffirmed the effect of the phase changes when the highest FAME yield was observed from two activated samples namely, Zn5_80 and Zn5_140. The optimized reactions condition of catalytic conversion of SO containing 10% OA at 5 °C/min heating rate, 3 wt % catalyst concentration, 30:1 methanol to oil molar ratio, reaction time of 100 °C for 2 h gave 92% FAME yield when Zn5_140 was used as the catalyst. The detected of the single phase of $Zn_5(OH)_8(NO_3)_2$ in Zn5_80, $Zn_5(OH)_8(NO_3)_2$ and ZnO in Zn5_140 (2-phase system), including $Zn_5(OH)_8(NO_3)_2$, $Zn_3(OH)_4(NO_3)_2$, and ZnO in Zn5_170 (3-phase system), suggested all three phases contributes to the high catalytic activity in methanolysis of the acidic oils. Both Zn5_140 and Zn5_170 gave a comparably high FAME yields based on statistical analyses. This study ascertained the synergistic effects of the high acidity (>0.4 mmol/g) and the dominant active phases of the thermally treated layered Zn hydroxide nitrate on the high catalytic activity that favours esterification of acidic oil feedstocks.

---

* Corresponding author.
  E-mail address: shangeetha@usm.my (S. Ganesan).

1. Introduction

Fatty acid methyl ester (FAME) commonly known as biodiesel, is a renewable and sustainable energy source, which can be produced via methanolysis of vegetable oils, animal fats, waste oils or greases, and fatty acid molecules in the presence of a catalyst [1]. Conventionally, FAME has been generated using a homogeneous catalyst due to the high reaction rate under mild conditions [2–5]. However, both homogenous transesterification or esterification reactions produce a single-phase product which is a mixture of glycerol/water and catalyst. Hence, the separation of FAME from the by-products is an important issue [1]. The presence of a homogeneous acid/base catalyst in the final FAME product is also less desirable as it can cause contamination to the engine. In recent years, research has focused on the development and investigation of metal oxides, metal hydroxides, and others [6–10].

Technologically promising properties of the layered hydroxyl salts (LHS) has garnered the interest of researchers in the field of heterogeneous catalysis. Effects of heat treatment on the enhancement of the catalytic activities of the different phases of LHS promote myriad uses in base-catalysed reactions like transesterification [11,12], epoxidation [13] and some esterification reaction [8]. Because of their tunable anion exchange properties by changing chemical species, layered hydroxyl salts (LHS) have also been investigated as an effective catalyst for FAME production [14]. Zinc hydroxide nitrate or $Zn_5(OH)_8(NO_3)_2 \cdot 2H_2O$, for example, has been reported by number of authors as the efficient solid catalyst for transesterification and esterification to produce high FAME yield [8,10]. It consists of nitrate anion stabilized between Zn hydroxide sheets octahedrally coordinated by hydroxyl anions. The zinc tetrahedron forms layers where a quarter of the octahedral sites remain vacant in between. The bases of the zinc tetrahedrons share hydroxyls with the octahedral sheet. While, the nitrate counterions are stabilized between the sheets, the water molecules occupy the apexes [10].

Reinoso et al. [15] reported the transesterification of soybean oil and methanol using zinc hydroxide nitrate catalyst (0.14 mmol/g of basicity). Soybean oil with 1.8×10^{-3} wt% of free fatty acids (FFA) without any pre-treatment and methanol were reacted with the catalyst in a 600 ml Parr reactor, with a diameter of 64 mm and equipped with a 4-angled blade stirrer. The fatty acid methyl ester (FAME) yield was determined by gas chromatography (GC) to be 51.5% and 76.8% for reaction temperatures of 100 °C and 140 °C, respectively, using 3 wt% of catalyst loading, 30:1 of methanol to oil molar ratio for 2 h [15]. Szabados et al. [12], in their most recent work, compared the feasibility of CaIn in transesterification of dimethyl carbonate with glycerol into glycerol carbonate with the performances of different types of metal (Ca, In, Al, Sc, V, Cr, Fe, Ga, Co, Zn, Mg, Ni) incorporated hydrotalcites. They found that all the synthesized hydrotalcites possessed very high reactivity with comparable recycling ability, further confirming the feasibility of other base catalysed reactions [12].

In another work, Zięba *et al*. [10], performed methanolysis of triacetin and castor oil as feedstocks at 50 °C and 60 °C, respectively, using 5 wt% of catalyst loading, and a methanol to oil ratio of 29:1 for 3 h under refluxing conditions in a 100 ml glass reactor under atmospheric pressure with stirring. Zinc hydroxide nitrate (Zn-5) catalyst was thermally treated at 105, 120, 140, 170, and 300 °C for 2 h prior to use for transesterification of triacetin compared to ZnO catalyst. After 3 h of reaction time, untreated Zn-5 catalyst gave the highest conversion yield, whereas Zn-5 thermally treated at 105, 120, and 140 °C showed a decreasing trend in catalytic activity with the increase in treatment temperature due to the formation of ZnO. This report shows that zinc hydroxide nitrate catalyst should not be treated at high temperatures to preserve the catalytic activity. In addition, transesterification of castor oil provided only 20% of FAME yield at 60 °C under the same conditions [10].

Zinc hydroxide nitrate has also been reported as a suitable catalyst for both transesterification of refined palm oil (RPO) and esterification of lauric acid. The reaction was carried out in a closed pressure vessel with varying types of alcohol, alcohol to oil molar ratios, catalyst loadings, and reaction temperatures. The esterification of lauric acid gave a high ester yield of more than 90% at 140 °C for 2 h. As for transesterification of RPO, 95.7% of methyl ester was obtained under a 48:1 methanol to oil molar ratio at 150 °C for 2 h [8]. Zinc hydroxide nitrate represents a unique property capable of transesterification and esterification reactions. Because of the thermal stability of $Zn_5(OH)_8(NO_3)_2 \cdot 2H_2O$, it has resulted in a new class of solid base catalysts known as layered hydroxide salts has been developed [16]. The recyclability and resistance to water [8] and FFA warrant an in-depth study.

Various forms of zinc hydroxide nitrate, derived from varying preparation methods, have been reported in recent years for application as catalysts for biodiesel synthesis. However, the different properties exhibited different abilities to react with the different feedstocks. Taking this into consideration, in the present work, the thermal stability of zinc hydroxide nitrate; $Zn_5(OH)_8(NO_3)_2 \cdot 2H_2O$ labelled as Zn5) was studied. Key factor that led to high FAME yields obtained from the methanolysis of neat soybean oil (or soybean oil mixed with oleic oil) were investigated. The thermal decomposition and morphology of Zn5 material were carefully analyzed by thermogravimetric curves, diffraction patterns, FTIR spectra, and electron microscopic images.

2. Experiments

2.1. Chemicals

Zinc nitrate hexahydrate ($Zn(NO_3)_2 \cdot 6H_2O$, AR grade) was supplied by Sigma-Aldrich. Sodium hydroxide (NaOH, pellet, AR grade) was traded by MERCK. Methanol (Honeywell, AR grade) was used without further purification. Refined soybean oil was obtained from a supermarket in Nakhon Pathom, Thailand. Oleic acid (GC grade) was purchased by Panreac. Chloroform-D ($CDCl_3$ + 0.05%v/v TMS + silver foil, AR grade) was acquired by Cambridge Isotope Laboratories.
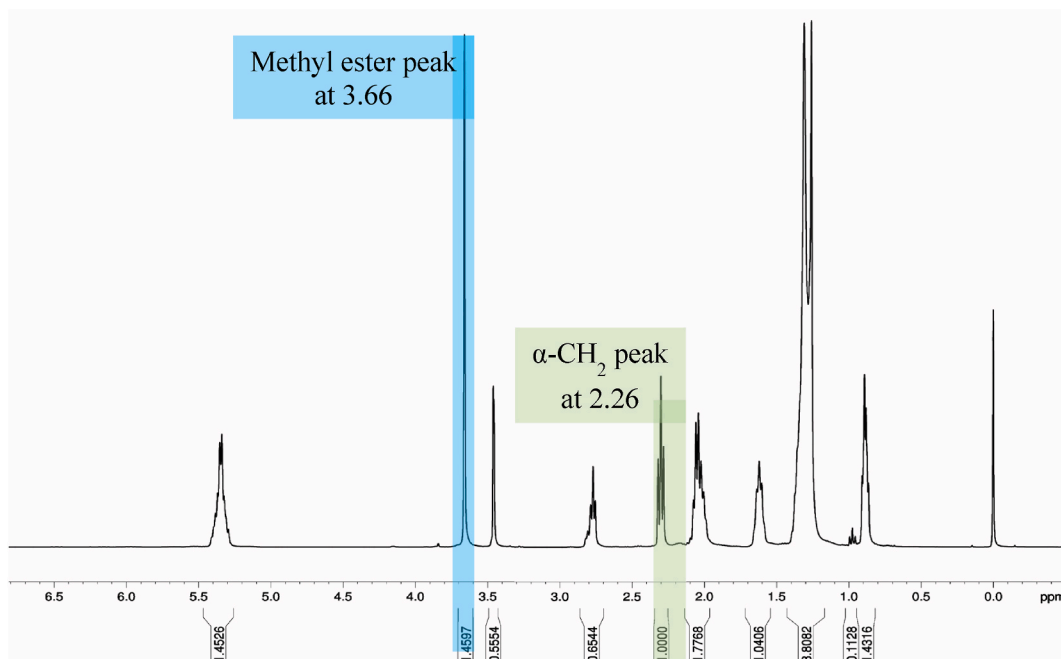
Fig. 1. Representative NMR spectra of methyl esters synthesized in this study.

2.2. Sample preparation

Zinc hydroxide nitrate was prepared by dropwise addition of 50 ml 0.75 M NaOH (aq) into 20 ml 3.5 M Zn(NO$_3$)$_2$ (aq) solution under vigorous stirring at room temperature. The obtained slurry was filtered, washed with DI water, and dried at 65 °C overnight, obtaining a white solid sample named Zn5. Thermal treated Zn5 samples were carried out by heating Zn5 at 5 °C/min to a specific temperature (70–170 °C) followed by an isothermal calcination at the above temperature for 5 h in a SNOL hot air oven furnace under ambient air conditions to obtain the samples; Zn5_y where y indicates the calcination temperature.

2.3. Sample characterizations

Phases of all prepared catalysts were identified by powder x-ray diffraction (PXRD), while their chemical composition, thermal decomposition, and morphology were studied by using, Fourier transformed infrared spectrometer equipped with attenuated total reflectance (FTIR-ATR) and a scanning electron microscope (SEM), respectively. Diffraction patterns were operated via a diffrac-tometer (Rigaku, Japan) equipped with a Cu K$_\alpha$, lamp at 40 kV and 35 mA in the 2-theta range of 5°–50°. FTIR-ATR spectra were measured on a spectrophotometer (Perkin Elmer) within the range of 4000 to 400 cm^{-1}, using 16 scans of accumulations at 4 cm^{-1} of resolution. Each sample was dried and coated with gold plasma prior to observation of the morphology on a microscope (SEM, Philips: XL30&EDAX) using a magnification of 20,000 at 15 kV. The basicity and acidity of the catalysts were determined using the benzoic acid and NaOH titration method with Hammett indicators.

2.4. Catalytic reaction activity

Zn5 and thermally treated Zn5 series were tested for the catalytic conversion of neat soybean oil or a mixture of 10% w/w oleic acid in soybean oil. The reaction was carried out in an ace-pressured tube using as a reactor equipped with a magnetic stirrer. Firstly, catalyst and methanol were mixed in the reactor and heated to the required temperature in oil bath under magnetic-stirrer (about 500 rpm) for 5 min. Then, the substrate was added into the mixture at a methanol-to-oil ratio of 30: 1 and 3 wt% of catalyst loading compared to oil for 2 h. After the required reaction time, the liquid layer was collected in 50 ml conical tube, and solid layer was removed. The methyl ester contents in the liquid layer were quantified and measured for conversion to biodiesel yield using ^{1}H NMR. The percent conversion of % FAME yields can be calculated using the equation given below [17]:

$$\% \text{ Methyl ester yield} = \frac{2A_{CH_3}}{3A_{CH_2}} \times 100\% \tag{1}$$

where A_{CH_3} and A_{CH_2} are the integration areas of NMR peaks corresponding to methyl esters (3.7 ppm) and methylene protons (2.3 ppm), respectively. The multiplication numbers of 2 and 3 are from 2 protons at the methylene carbon in triglycerides (free fatty acids) and 3 protons at the methyl carbon in methyl ester, respectively. A representative NMR spectrum of the methyl esters produced in this

Table 1
Acidity and basicity of Zn5 range of catalysts.

Catalyst	Acidity[a] (mmol/g)	S.D. Acidity	Basicity[b] (mmol/g)	S.D. Basicity
Zn5	0.14	0.19	0.12	0.30
Zn5-R5_70 °C	0.32	0.05	0.16	0.09
Zn5-R5_80 °C	**0.48**	0.11	0.15	0.03
Zn5-R5_90 °C	0.14	0.09	0.17	0.07
Zn5-R5_100 °C	0.32	0.09	0.19	0.07
Zn5-R5_120 °C	0.30	0.09	0.12	0.03
Zn5-R5_140 °C	**0.40**	0.06	0.11	0.02
Zn5-R5_170 °C	**0.46**	0.06	0.10	0.03
ZnO	0.13	0.04	0.14	0.03

[a] Phenolphthalein.
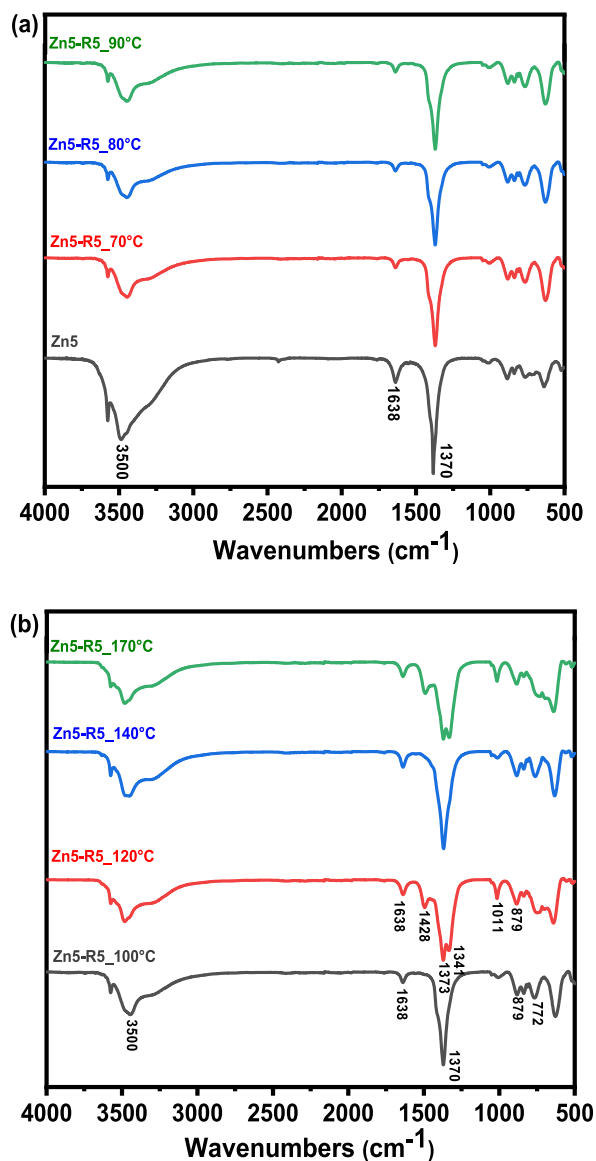[b] Methyl red for Hammet indicators.

Fig. 2. FTIR spectra of (a) Zn5 and of thermally treated Zn5 at 70, 80, 90 °C and (b) 100, 120, 140, 170 °C.
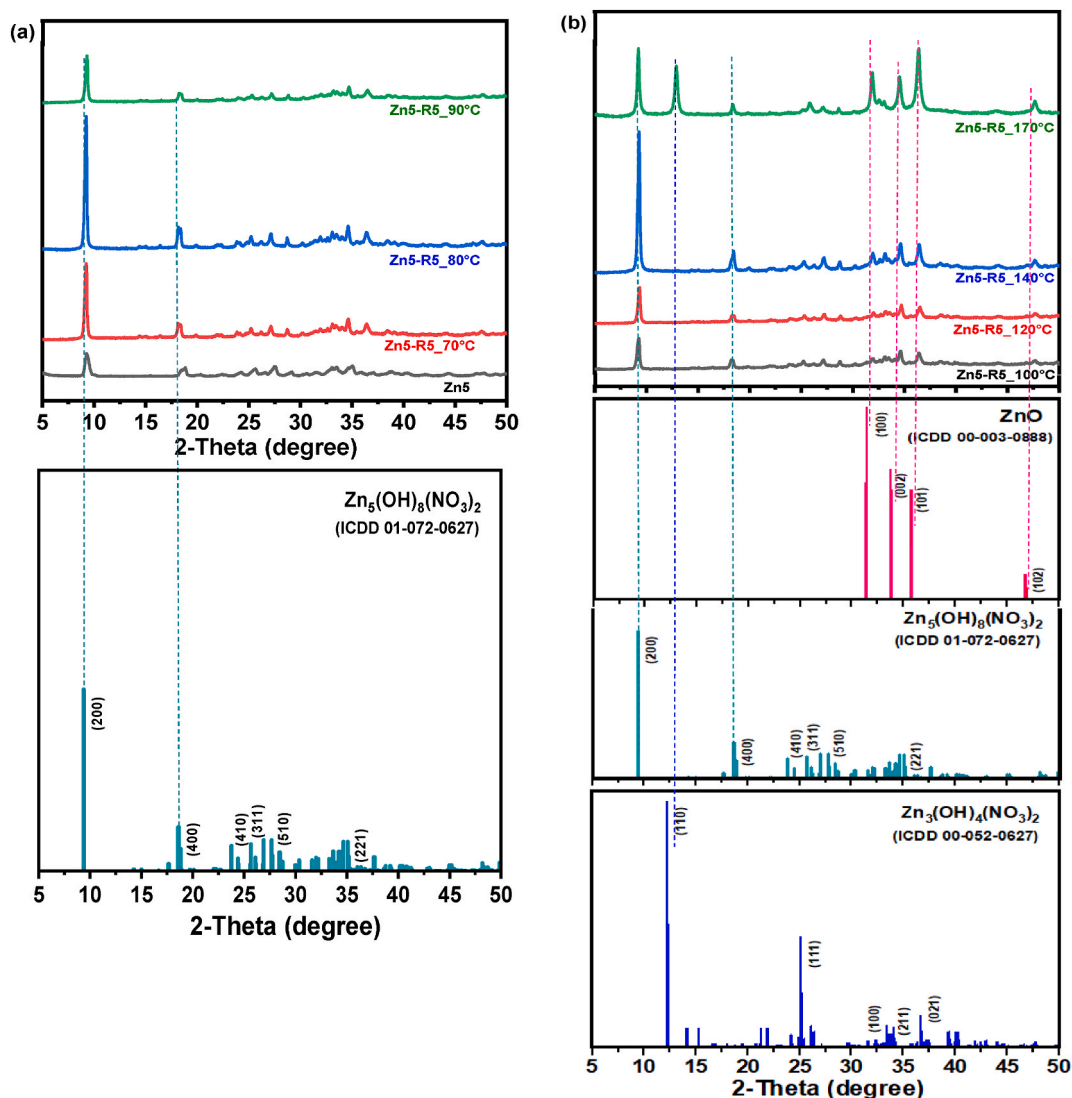
Fig. 3. XRD of (a) Zn5 and thermally treated Zn5 at 70, 80, 90 °C and (b) 100, 120, 140, 170 °C.

study is shown in Fig. 1.

The results of methyl ester yields were reported as the mean value and standard deviation (SD). Using version 18 of the predictive analytics software (PASW) application, descriptive statistics were computed. The methyl ester yield obtained under each reaction setting was evaluated using one-way analysis of variance (ANOVA), followed by Duncan's multiple range test to determine statistical significance. (p-values <0.05).

3. Results and discussion

3.1. Catalyst characterizations

As the main goal of this work is to find out how thermal treatment of catalyst affects the amount of methyl esters made when SO-containing OA is converted by catalysis, it is important to look more closely at the properties of the different catalysts obtained. The catalysts being studied include Zn5, Zn5_70 °C, Zn5_80 °C, Zn5_90 °C, Zn5_100 °C, Zn5_120 °C, Zn5_140 °C and Zn5_170 °C, which were characterised for acidity/basicity, functional group analysis through FTIR, crystallinity and phase study through XRD, and catalyst morphology through SEM.

3.1.1. Acidic/basic strength of catalysts

All the catalysts were estimated for basicity and acidity by titration with benzoic acid and NaOH solutions, respectively. As shown

in Table 1, the highest acidity was found in Zn5_80, while the highest basicity was found in Zn5_70. There appears to be a general trend toward increasing acidity and decreasing basicity at the activation temperatures above 90 °C. The highly acidic catalysts have an acidity of 0.4 or above (listed in bold in Table 1). Benzoic acid titration estimates the basic sites in the presence of the indicator as per NaOH for acidic sites. The titration estimates the total basicity and acidity of the solid catalysts [15]. The acidity of the catalysts in this study was found to be higher than the basicity, indicating the ability of the catalyst to participate in both esterification and transesterification reactions. However, the prominence of the acidity over the basicity shows the affinity of the reaction towards the esterification reaction as compared to the transesterification reaction. The acidic/basic strength of the catalyst was found to be closely related to the change in phase of the catalyst with thermal treatment (Fig. 3). Acidity was found to increase with thermal treatment until 80 °C and decrease at the phase change at 90 °C. The trend increases again until 140 °C which is the second point of phase change. At 170 °C the acidity continued to increase as HNO_3 was also formed as the decomposition product.

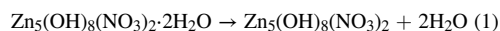### 3.1.2. Functional group analysis of the catalysts

Functional group analysis of the synthesized Zn5 exhibits a prominent band at 1370 cm^{-1}, which is attributed to the NO_2 stretching mode of the free nitrate ion as shown in Fig. 2(a and b). The band falls in the characteristic range of 1000–1500 cm^{-1} for nitrate stretching range confirming the successful synthesis of the zinc nitrate hydroxide catalyst. Subsequently, the catalysts ranging from Zn5_70 to Zn5_100 show a strong band at 1370 cm^{-1} assigned to free NO_2 stretching. However, the band splits into 1341 and 1370 cm^{-1} for the catalyst treated at 120 °C suggesting coordination of nitrate to Zn-cation. The trend was observed in all the catalysts treated above 100 °C. The fingerprint region shows other nitrate absorption bands appearing at *ca.* 722 cm^{-1} of symmetric deformation and near 829 cm^{-1} of asymmetric deformation. Another weak band at 1050 cm^{-1} is due to *N*-O stretching for the free nitrate group was found in Zn5 until Zn5_100. After which, the band become stronger and sharper, indicating an interesting change in bonding and suggesting the formation of unidentate coordinated nitrate in the catalyst [18].

The spectral region of OH stretching vibrations in all the synthesized catalysts exhibits a wide band at 3000 to 3750 cm^{-1}. The gradual structural change in the catalyst with thermal treatment is clearly visible in this region consisting of band attributed to layer hydroxyl layers and hydrogen bonds of the layer hydroxyl, water molecules and nitrate groups. The wide and sharp band shows a diminishing intensity with the increase in thermal treatment temperature. Another band stretching at 1011 cm^{-1} shows a gradual change from weak and wide to sharp and strong with the increase in the thermal treatment. The band, associated with the OH bending mode in Zn-OH species [18], becomes especially sharper and stronger after 120 °C. A sharp band at 1638 cm^{-1} attributed to bending vibrations of interlayer water molecules can be seen to also diminish in intensity with the increase in the temperature of thermal treatment. The FTIR spectral analysis of the catalysts from Zn5 to Zn5_170 °C corroborates well with the previously reported work on the use of $Zn_5(OH)_8(NO_3)_2 \cdot 2H_2O$ in transesterification of triglycerides [10].

3.1.3. Crystallinity of catalysts

The phase changes in the Zn5 catalysts with thermal treatment were also well observed in the PXRD analysis of the catalysts. Form Fig. 3 (a and b), the presence of $Zn_5(OH)_8(NO_3)_2$ can be clearly seen for the catalysts ranging from Zn5 to Zn5_170. Starting from Zn5_140 to Zn5_170 the peaks assigned to ZnO started to become more prominent. The PXRD showed three main distinctive diffraction patterns affiliated to $Zn_3(OH)_4(NO_3)_2$ $Zn_5(OH)_8(NO_3)_2$, and ZnO which corresponds well to the structures reported in previous studies [10,19,20]. Below the treatment temperature of 90 °C, the intensity of diffraction peaks are less prominent and they are mostly associated with $Zn_5(OH)_8(NO_3)_2$. Between temperatures of 140 °C–170 °C, diffraction peaks of $Zn_3(OH)_8(NO_3)_2$ started appearing and became more prominent as temperature increases suggesting the slow decomposition of Zn5 compound. At 170 °C, ZnO diffraction peaks were increasingly evident while the characteristic peaks of $Zn_5(OH)_8(NO_3)_2$ were possibly suppressed by the appearance of ZnO peaks in the same 2-theta range. A simultaneous presence of all three compounds were observed at 170 °C as per previous reports [18, 20]. When Zn5 is heated above 100 °C, water is expelled causing the migration of interlayer nitrate ions to replace the lost water and form anhydrous $Zn_5(OH)_8(NO_3)_2$ [18,21]. Thus, heat treatment resulted in the conversion of hydrated Zn5 to anhydrous Zn5. The interlayer nitrate ions are more tightly bound in the anhydrous Zn5 form because it is within the coordination sphere of Zn^{2+}. Further increase in temperature promotes dehydroxylation forming the other two species, $Zn_5(OH)_4(NO_3)_2$ and ZnO. Moezzi et al. [20] reported that there was no reduction in the interlayer separation as the treatment temperature was increased, suggesting a constant water content in between the layers with only monotonic thermal expansion.

The observation in Fig. 3 suggests processes (1), (2), and (3) occurring with the increase in temperature from Zn5 to Zn5_90, Zn5_100 to Zn5_140 and Zn5_170, respectively.

$$Zn_5(OH)_8(NO_3)_2 \cdot 2H_2O \rightarrow Zn_5(OH)_8(NO_3)_2 + 2H_2O \quad (1)$$

$$Zn_5(OH)_8(NO_3)_2 \rightarrow Zn_3(OH)_4(NO_3)_2 + 2ZnO + 2H_2O \quad (2)$$

$$Zn_3(OH)_4(NO_3)_2 \rightarrow 3ZnO + 2HNO_3 + 2H_2O \quad (3)$$

In the first (1) step, hydration water was lost and the peaks of $Zn_5(OH)_8(NO_3)_2$ started appearing and became more distinct as temperature increased. The second step (2) shows the formation of ZnO and $Zn_3(OH)_4(NO_3)_2$ through de-hydroxylation which are observed in the diffraction pattern in this study. Step (3) shows further decomposition, forming ZnO. The sharp diffraction pattern of ZnO is well formed in Zn5_170 as can be observed in Fig. 3, while still containing considerable amounts of $Zn_5(OH)_8(NO_3)_2$ and $Zn_3(OH)_4(NO_3)_2$. Table 2 lists the 2-theta values for the active species produced with each phase change as compared to the previous study. It was found that the compounds are well detected and confirmed to be formed at the corresponding phase change stage in this

Table 2
Identification of active species in this work as compared to previous study.

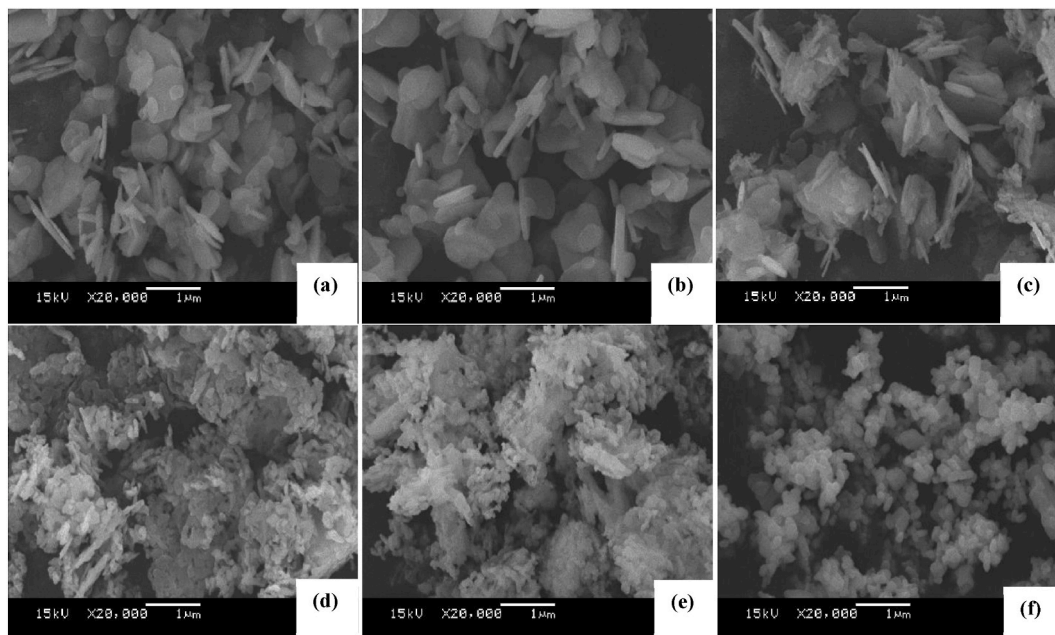| Assignment	2-Theta (degree)	
	This work	[10]
$Zn_5(OH)_8(NO_3)_2$	9.2, 18.3, 27.1, 34.5	9.1, 18.2, 25.1, 26.9, 28.5, 32.5, 33.0, 34.5
$Zn_3(OH)_4(NO_3)_2$	12.9, 27.1, 31.9, 34.5	12.8, 25.7, 31.8, 32.5, 34.4, 43.8
ZnO	31.9, 34.5, 36.3, 47.5	31.8, 34.4, 36.2

Fig. 4. SEM images of calcination of Zn5 at (a) 80, (b) 90, (c) 100, (d) 120, (e) 140, (f) 170 °C.

study.

3.1.4. Surface morphology of the catalysts

The morphology changes of the Zn5 and thermally treated catalysts were studied by SEM. Fig. 4 reveals the Zn5 before thermal treatment has a plate-like structure, which can be seen to reorganize as the temperature of treatment is increased. The structure turns from plate-like (80–90 °C) to spongy clusters (100–140 °C) to spherical particles (170 °C). Fig. 4(c) has small areas of spongy clusters. The observation of the appearance of spherical particles at 170 °C corresponds to the start of the formation of ZnO as reported by Zieba et al. [10]. Notably, ZnO as a commercially available reference, was reported to be highly crystalline with large particles aligned in one direction. This differs with ZnO formation from the thermal decomposition of Zn5 where a mixture of amorphous and crystalline phases are obtained [10]. As implied by the results in Fig. 4(a–f), the formation of ZnO began at around 90 °C.

3.2. Effects of thermal stability of catalysts on methyl esters yields

The catalytic activity of Zn5 and thermally treated Zn5_70 to Zn_170 in soybean oil (SO) containing 10% oleic acid (OA) at 3% catalyst loading, and a 30:1 methanol to oil molar ratio at 100 °C for 2 h reaction time was studied against pure SO. The results in Fig. 5 (a and b) show that methanolysis of SO containing 10% OA gave higher FAME yields than that of pure SO. The low basicity of all catalysts (Table 1) matched well with the low FAME yields derived from pure SO, which showed that, for each catalyst, the trans-esterification limit had been reached. By using the acidic oil feedstocks, simultaneous transesterification of triglycerides and esterification of FFA took place, resulting in increased FAME yields. The highest FAME yield was obtained at Zn5_140. Interestingly, there seems to be a cluster effect that corresponds to the phase changes in the thermally treated catalyst. This observation can be explained by the change in phase of thermally treated Zn5 as seen in Figs. 2–4. For 10% OA containing SO, the range of catalysts from Zn5 to Zn5_80 (containing $Zn5(OH)_8(NO_3)_2$ phase) shows an increasing trend in FAME yield. The methyl esters yield dips at Zn5_90 and slowly increases to peak at Zn5_140 (due to the copresence of $Zn5(OH)_8(NO_3)_2$ and ZnO). Then, the methyl esters yield (mean value) decreases slightly by using Zn5_170. From statistical analysis, although the competitive $Zn_3(OH)_4(NO_3)_2$ phase formed in the Zn5_170, it has very little effect to esterification efficiency compared to that of Zn5_140 (insignificantly different; $p \leq 0.05$). The different phases,
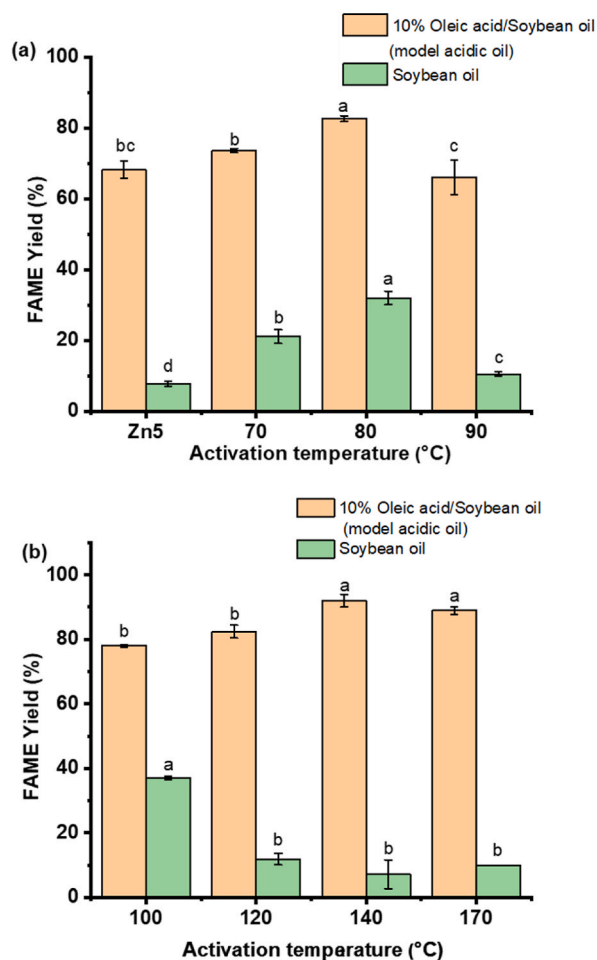
Fig. 5. FAME yield (%) of 10% oleic/soybean oil and soybean oil catalysed by Zn5 and activated Zn from 70 to 170 °C, heating rate of 5 °C/min, 3% catalyst loading using, 30:1 of MeOH to oil ratio at 100 °C for 2 h [The labels a, b and c refers to the group classification given based on statistical analyses (significantly different; $p \leq 0.05$)].

as highlighted in Equations (1)–(3) contributes to the corresponding change in the catalytic activity of the catalyst. The diffraction pattern of Zn5 is weak and distorted as compared to the sharper peaks observed with the thermally treated Zn5_70 and Zn5_80. The active species is $Zn_5(OH)_8(NO_3)_2$, at these two temperatures, explaining the catalyst's high acidity (>0.4 mmol/g). The prominence of the active species can be observed from the diffraction patterns in Fig. 2, where the peak is more prominent in Zn5_80. This clearly supports the results for a higher methyl ester yield for Zn5_80. The Zn5_90 peaks corresponding to $Zn_5(OH)_8(NO_3)_2$ shows signs of weakening with less intensity which corresponds to the reduction in methyl ester yield. This is due to the phase change described in equation (1) as water is lost, resulting in the $Zn_5(OH)_8(NO_3)_2$ formation. The relatively low FAME yields obtained from the Zn5_90 (compared to Zn5_80) reflects some conversion of $Zn_5(OH)_8(NO_3)_2$ to ZnO as monitored by the SEM image (Fig. 4(c)). However, it is quite possible that the amount of ZnO present in the Zn5_90 may be lower than the detection limit of diffractometer. As a result, the gradual formation of ZnO phase is responsible for the decreased acidity of the Zn5_90, which corresponds to a decreased FAME yield since low acidic catalysts (0.14 mmol/g) are less favourable to esterification than $Zn_5(OH)_8(NO_3)_2$.

The intensity of the diffraction picks up at Zn5_100, indicating the removal of water, hence an increase in methyl ester yield was observed. As temperature increases up to 170 °C, de-hydroxylation forms more $Zn_3(OH)_4(NO_3)_2$. The subsequent increase in the acidity of the catalyst from Zn_100 to Zn_170 also corresponds well with the increased ZnO content, and the increase in the methyl esters yield as per Fig. 5(b). Further increased activation temperature resulted in the formation of new phase, $Zn_3(OH)_4(NO_3)_2$. Consequently, the competitively formed $Zn_3(OH)_4(NO_3)_2$ phase in the Zn5_170 did not give any adverse effects on the FAME yields, being quite similar to that obtained from the Zn5_140.

Note that all catalysts showed very low activity for the transesterification of soybean oil (SO). This is also expected given that the basicity of the catalysts was found to be very low as compared to their acidity. During the 2-h reaction time in the oleic acid/soy bean oil mixed system, the triglycerides, in addition to undergoing transesterification, are partially hydrolysed to free fatty acids and esterified together with the oleic acid, resulting in a significantly higher yields for the mixed system. During the esterification of the
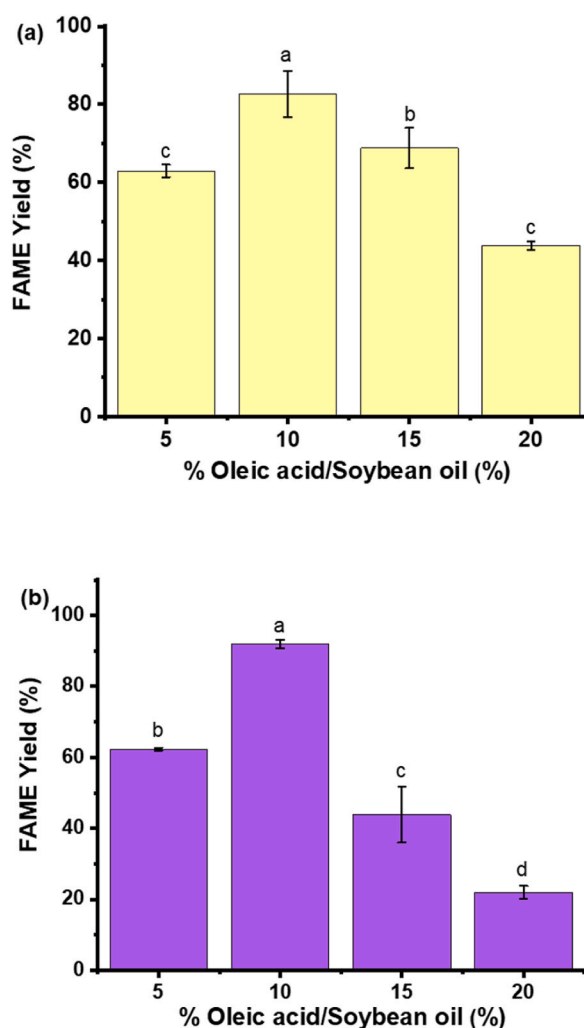
Fig. 6. FAME yield (%) of 5–20% Oleic/Soybean oil catalysed by a) Zn5_80 and b) Zn5_140 °C with heating rate of 5 °C/min, 3% catalyst loading using, 30:1 of MeOH to oil ratio at 100 °C for 2 h [The labels a, b, c and d refers to the group classification given based on statistical analyses (significantly different; $p \leq 0.05$)].

pure oleic acid, water is produced which in turn hydrolyses the triglycerides of soy bean oil into free fatty acids [22]. The free fatty acids are available for esterification by the Zn catalysts, hence the higher yield observed for the mixed system. This observation corresponds to the highly acidity of the thermally activated Zn5 catalysts, and three active phases, $Zn_5(OH)_8(NO_3)_2$, $Zn_3(OH)_4(NO3)_2$, and the sufficient ZnO content, that favour esterification.

Due to the significantly FAME yield results (mean values) obtained at the two hypothesized phase change points, Zn5_80 and Zn5_140, the subsequent investigations were carried out only for these two types of catalysts for the optimization of reaction parameters. The catalytic activity of Zn5_80 and Zn5_140 in the presence of free fatty acid content were studied by reacting various mixtures of soybean oil (SO) with oleic acid (OA) from 5% to 20% at 100 °C for 2 h at a catalyst loading of 3 wt% and a methanol to oil molar ratio of 30:1. Fig. 6(a and b) shows the maximum tolerance of FFA in soybean to give a high FAME yield for both catalysts at a 10% OA mixture in SO. One notable observation from this study, is the ability of the thermally treated Zn5 to esterify SO with OA up to 10%. This can be explained by the Lewis acid property of Zn. The carbonyl oxygen of the oleic acid reacts with the zinc ion, acting as a Lewis acid, forming a carbocation susceptible to nucleophilic attack by methanol. A tetrahedral intermediate is formed, and water is eliminated to form 1 mol of methyl ester. The efficiency of Lewis acid based metal catalysts in esterification reactions has been well studied and reported over the years [9,23,24].

Cordeiro et al. [8] studied the esterification of lauric acid and the transesterification of refined palm oil in separate experiments, and reported high FAME yields for the individual processes using zinc hydroxy nitrate (ZHN) as catalyst. They hypothesized that during the esterification reaction, the nitrate ions in the catalyst interchanged with laurate ions. Hence, the swelling of the crystallites gave access to the reagents to reach the catalytic sites located on the surface and edges of the layered crystal structure. Table 3 highlights the underlying cause for the high FAME yield obtained by using the thermally activated Zn5 at varied temperatures.

Table 3

The underlying reason for the high FAME yield obtained by thermally activating Zn5 at different temperatures.

| Activation temp. (°C)	Phase	Reason for high FAME yields
≤ 80	1-phase system $Zn_5(OH)_8(NO_3)_2$	The acidity increases as the activation temperature rises.
90–140	2-phase system $Zn_5(OH)_8(NO_3)_2$ ZnO	Sufficiently higher ZnO content resulted in an increase in acidity.
170	3-phase system $Zn_5(OH)_8(NO_3)_2$ ZnO $Zn_3(OH)_4(NO_3)_2$	Sufficiently higher ZnO content resulted in an increase in acidity. $Zn_3(OH)_4(NO_3)_2$ exhibited no negative effects on the esterification activity.
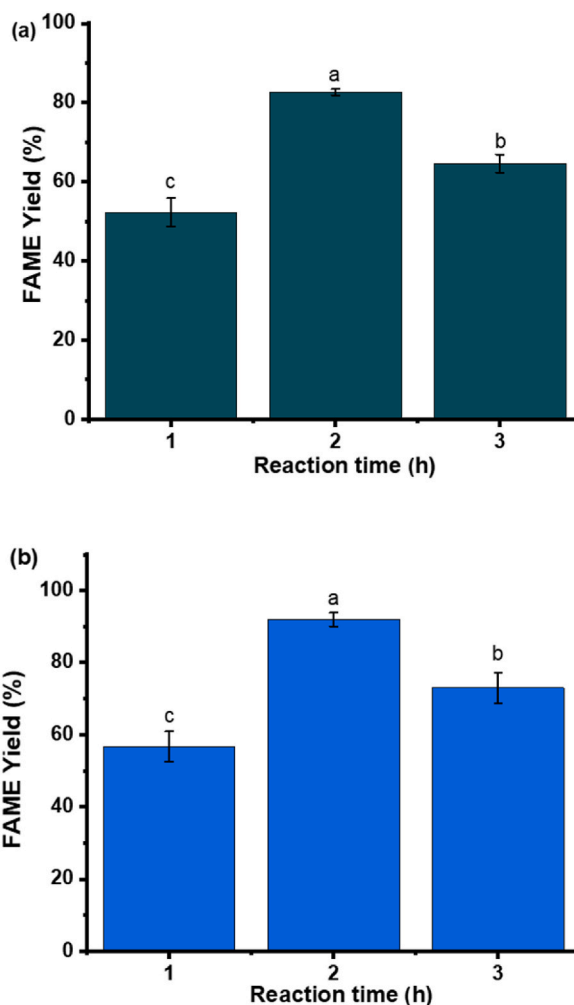
Fig. 7. FAME yield (%) of 10% Oleic/Soybean oil catalysed by a) Zn5_80 and b) Zn5_140 °C with heating rate of 5 °C/min, 3% catalyst loading using, 30:1 of MeOH to oil ratio at 100 °C for 1–3 h [The labels a, b and c refers to the group classification given based on statistical analyses (significantly different; $p \leq 0.05$)].

A study of the best reaction time for the esterification reaction was conducted with Zn5_80 and Zn_140 at 3% catalyst loading using, 30:1 methanol to oil ratio at 100 °C for 1–3 h. It was determined that 2 h is sufficient to give the highest FAME yield for both types of catalysts tested, as seen in Fig. 7(a) and b. A further increase to 3 h shows a decline in the FAME yield due to the thermal degradation of the FAME produced after a prolonged period of heating. A comparison of the yield reported over the years for other layered metal hydroxides shows that the optimum reaction time to give the highest FAME yield lies between 2 and 3 h depending on the type of catalysts and feedstock. Liu et al. [33] found that when anhydrous poultry fat and methanol were transesterified at a prolonged reaction time, the yield of FAME decreased even though the ratio of methanol to oil stayed the same.
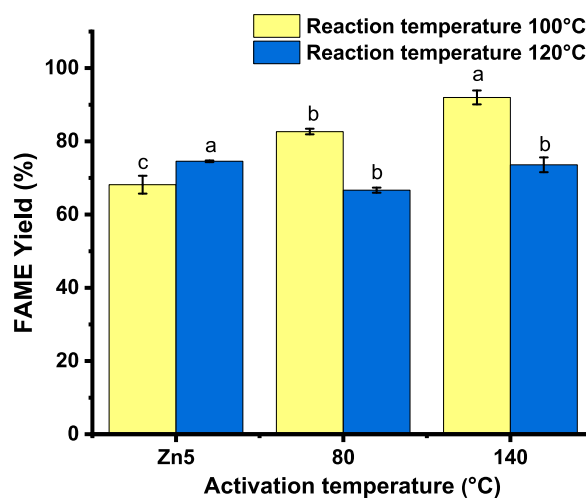
Fig. 8. FAME yield (%) of 10% Oleic/Soybean oil catalysed by Zn5, Zn5_80 and Zn5_140 °C with heating rate of 5 °C/min, 3% catalyst loading using, 30:1 of MeOH to oil ratio at 100 °C and 140 °C for 2 h [The labels a, b and c refers to the group classification given based on statistical analyses (significantly different; $p \leq 0.05$)].

Table 4
Summary of the reaction conditions for layered metal hydroxides catalysed FAME production with various feedstock.

Catalysts	Feedstock	Reaction conditions				Yield (%)
		Catalyst (wt%)	MeOH:oil	Temp (°C)	Time (min)	
Zinc hydroxide nitrate (From this work)	Soybean oil	3	30:1	100	120	37.5
		3	30:1	140	120	43.8
		10	30:1	140	120	98.9
	10% oleic acid/soybean oil	3	30:1	140	120	97.8
		3	30:1	120	120	95.4
		3[a]	30:1	100	120	96.7
Zinc hydroxide nitrate [15]	Soybean oil	3	30:1	100	120	51.5
		3	30:1	140	120	76.8
Zinc hydroxide nitrate [8]	Lauric acid	4	4:1	140	120	96.2
		6	2:1	140	120	95.6
		6	6:1	140	120	95.7
	Palm oil	6	48:1	150	120	95.7
Zinc hydroxide nitrate [6]	Triacetin	5	29:1	50	180	70.0
Calcined Mg-Al hydrotalcite [25]	Soybean oil	0.04	50:1	200	4	95.9
Calcined-rehydrated Mg-Al hydrotalcite [26]	Sunflower oil	10	12:1	60	2	56
Calcined Ca-Mg-Al hydrotalcite [27]	Microalgae oil	3	6:1	65	5	90
Calcined hydrotalcites	Soybean oil	5	12:1	200	60	96.0
MgO-Al (from Mg(NO$_3$)$_2$)		5	12:1	200	60	95.0
MgO-Al (from Mg(OH)2)		5	12:1	200	60	80.0
MgO-Al (from (MgCO$_3$)$_4$*Mg(OH)$_2$) [28]		5	12:1	200	60	99.0
Mg-Al hydrotalcites [29]	Tributyrin	0.6	30:1	60	1200	82.0
Mg-Al hydrotalcites [30]	Refined rape oil	1.5	6:1	65	240	90.5
Mg-Al hydrotalcites [31]	Tributyrin	1.7	30:1	60	180	74.8
Mg-Al hydrotalcites [32]	Soybean oil	7.5	15:1	60	540	66.0
Mg-Al hydrotalcites [33]	Anhydrous poultry fat	10	6:1	120	2640	76.0
		10	15:1	120	900	80.0
		10	30:1	120	420	82.0
		10	60:1	120	180	84.0
		10	60:1	120	360	94.0
K-Mg-Al hydrotalcites [34]	Palm oil	7.5	30:1	100	360	96.9
Mg-Al-NO3 hydrotalcites	Soybean oil	5	55:1	130	420	70.0
Zn-Mg-Al-NO3 hydrotalcites [35]		5	55:1	130	420	64.0
Mg-Al-CO3 hydrotalcites [36]	Cottonseed oil	1	6:1	200	540	80.0
Mg-Al hydrotalcites [37]	Canola oil	3	6:1	60	540	71.9
Mg-Ca oxides [38]	Sunflower oil	2.5	12:1	60	180	95.0
Li-Al LDH [39]	Tributyrin	3	30:1	65	180	98.0
	Soybean oil	1	15:1	65	120	83.1

The catalysts in this study were then explored for the efficiency of the reaction at two different reaction temperatures, namely 100 °C and 120 °C. The experiment was conducted for Zn5, Zn5_80, and Zn5_140 as the representative catalysts at the same catalytic loading and methanol to oil molar ratio for 2 h as shown in Fig. 8. Zn5_140 was found to give the highest yield at a reaction temperature of 120 °C, with a consistently higher yield than Zn5 and Zn5_80. Table 4 gives a summary of the reaction conditions for layered metal hydroxides catalysed FAME production with various feedstocks. It is interesting to note that most of the prepared layered metal hydroxides reported focused on utilizing base catalyst for transesterification of triglycerides. Very few works reported the optimization of free fatty acids containing oils as per this current study. The results of this study prove that the ZHN catalyst is more effective as an acidic catalyst for esterification reactions as compared to basic catalysts for transesterification reaction. Reinoso et al. [11] investigated only the transesterification ability of ZHN, while Cordeiro et al. [8] reported a higher esterification activity of ZHN similar to this study. This reiterates the importance of this work in exploring in depth the effects of thermal treatment of the Zn5 layered hydroxide in the esterification reaction to produce FAME.

4. Conclusions

The present study demonstrates that the thermally treated layered Zn hydroxide nitrate at 80 and 140 °C is more prevalent in terms of catalytic acidity, which in turn greatly contributes to the esterification of the 10 wt% OA containing SO. At the same optimized reaction conditions, the methyl ester yield of Zn5_140 was 92%, which was higher than that of Zn5_100. This can be attributed to the formation of the acidic $Zn_3(OH)_4(NO_3)_2$ and ZnO active phases, which promote efficient esterification processes. The characterization and optimization results also reaffirm that the main reaction taking place in the reaction medium is the esterification reaction even though triglycerides were present at 90 wt% in the form of SO. During the course of the 2-h reaction, the triglycerides partially transesterified to methyl ester, and also hydrolysed into FFA which is then esterified to methyl esters. This is the first study to examine the effects of thermal treatments and subsequent changes of the acidity and phase of layered zinc hydroxide nitrate and the esterification of high FFA soy bean oil. Future works can be emphasized on further characterization and optimization of the Zn_80 and 140 °C which showed the most prevalent catalytic activity for esterification and transesterification reaction.

Author contribution statement

Siwaporn Meejoo Smith: Conceived and designed the experiments, Analyzed and interpreted the data, Contributed reagents, materials, analysis tools or data, Wrote the paper.
Wilasinee Lerdrittipong: Conceived and designed the experiments, Performed the experiments, Analyzed and interpreted the data, Wrote the paper.
Warisara Woranuch: Performed the experiments, Analyzed and interpreted the data, Wrote the paper.
Suwilai Chaveanghong: Conceived and designed the experiments, Analyzed and interpreted the data.
Shangeetha Ganesan: Conceived and designed the experiments, Analyzed and interpreted the data, Wrote the paper.

Data availability statement

Data included in article/supp. material/referenced in article.

Declaration of competing interest

The authors declare that they have no known competing financial interests or personal relationships that could have appeared to influence the work reported in this paper

Acknowledgements

References

[1] V. Mandari, Santhosh, K. Devarai, Bioenergy Res. 1 (2021) 3.
[2] R. Jambulingam, R. Srinivasan Gokul, S. Palani, M. Munir, Muhammad Saeed, A. Mohanam, S.N. Gokul, Appl. Sci. 2 (2020) 1454.
[3] Z. Abelniece, L. Laipniece, V. Kampars, Biomass Conver. Bioref. 2020 (2020) 1–9.
[4] L. Gu, W. Huang, S. Tang, S. Tian, X. Zhang, Chem. Eng. J. 259 (2015) 647–652.
[5] B. Kim, H. Im, J.W. Lee, Bioresour. Technol. 185 (2015) 421–425.
[6] A. Zięba, A. Pacuła, A. Drelinkiewicz, Energy Fuel. 24 (2009) 634–645.
[7] D.M. Reinoso, M.B. Fernandez, D.E. Damiani, G.M. Tonetto, Int. J. Low Carbon Technol. 7 (2012) 348–356.
[8] C.S. Cordeiro, G.G.C. Arizaga, L.P. Ramos, F. Wypych, Catal. Commun. 9 (2008) 2140–2143.
[9] M. Melchiorre, M.E. Cucciolito, M. di Serio, F. Ruffo, O. Tarallo, M. Trifuoggi, R. Esposito, ACS Sustain. Chem. Eng. 9 (2021) 6001–6011.

[10] A. Zięba, A. Pacuła, E.M. Serwicka, A. Drelinkiewicz, Fuel 89 (2010) 1961–1972.

[11] B.M. Choudary, M. Lakshmi Kantam, C. Venkat Reddy, S. Aranganathan, P. Lakshmi Santhi, F. Figueras, J. Mol. Catal. Chem. 159 (2000) 411–416.

[12] M. Szabados, A. Adél Ádám, P. Traj, S. Muráth, K. Baán, P. Bélteky, Z. Kónya, Á. Kukovecz, P. Sipos, I. Pálinkó, J. Catal. 391 (2020) 282–297.

[13] C. Shen, J. Ma, T. Zhang, S. Zhang, C. Zhang, H. Cheng, Y. Ge, L. Liu, Z. Tong, B. Zhang, Appl. Clay Sci. 187 (2020), 105478.

[14] N. Thomas, Mater. Res. Bull. 47 (2012) 3568–3572.

[15] D.M. Reinoso, D.E. Damiani, G.M. Tonetto, Catal. Sci. Technol. 4 (2014) 1803–1812.

[16] T. Biswick, W. Jones, A. Pacuła, E. Serwicka, J. Podobinski, J. Solid State Chem. 180 (2007) 1171–1179.

[17] G. Knothe, 5 77, J. Am. Oil Chem.ʾ Soc. 2000 77 (2000) 489–493.

[18] C. Chouillet, J.M. Krafft, C. Louis, H. Lauron-Pernot, Spectrochim. Acta Mol. Biomol. Spectrosc. 60 (2004) 505–511.

[19] A. Gordeeva, Y.J. Hsu, I.Z. Jenei, P.H.B. Brant Carvalho, S.I. Simak, O. Andersson, U. Haüssermann, ACS Omega 5 (2020) 17617–17627.

[20] A. Moezzi, P.S. Lee, A.M. McDonagh, M.B. Cortie, J. Solid State Chem. 286 (2020).

[21] S.R. Tavares, V.S. Vaiss, F. Wypych, A.A. Leitão, Appl. Clay Sci. 114 (2015) 103–111.

[22] D. Kusdiana, S. Saka, Bioresour. Technol. 91 (2004) 289–295.

[23] P.-L. Boey, S. Ganesan, G.P. Maniam, M. Khairuddean, J. Efendi, Energy Convers. Manag. 65 (2013).

[24] S. Ganesan, S. Nadarajah, M. Khairuddean, G.B. Teh, Renew. Energy 140 (2019).

[25] M.S. Dhawan, S.C. Barton, G.D. Yadav, Catal. Today 375 (2021) 101–111.

[26] E. Dahdah, J. Estephane, Y. Taleb, B. el Khoury, J. el Nakat, S. Aouad, Sustain Chem Pharm 22 (2021), 100487.

[27] E.E. Çakırca, A.N. Akın, Sustain. Chem. Pharm. 20 (2021), 100378.

[28] M. di Serio, M. Ledda, M. Cozzolino, G. Minutillo, R. Tesser, E. Santacesaria, Ind. Eng. Chem. Res. 45 (2006) 3009–3014.

[29] Y. Xi, R.J. Davis, J. Catal. 254 (2008) 190–197.

[30] H. yan Zeng, Z. Feng, X. Deng, Y. qin Li, Fuel 87 (2008) 3071–3076.

[31] D.G. Cantrell, L.J. Gillie, A.F. Lee, K. Wilson, Appl. Catal. Gen. 287 (2005) 183–190.

[32] W. Xie, H. Peng, L. Chen, J. Mol. Catal. Chem. 246 (2006) 24–32.

[33] Y. Liu, E. Lotero, J.G. Goodwin, X. Mo, Appl. Catal. Gen. 331 (2007) 138–148.

[34] W. Trakarnpruk, S. Porntangjitlikit, Renew. Energy 33 (2008) 1558–1563.

[35] W.M. Antunes, C. de O. Veloso, C.A. Henriques, Catal. Today 133–135 (2008) 548–554.

[36] N. Barakos, S. Pasias, N. Papayannakos, Bioresour. Technol. 99 (2008) 5037–5042.

[37] O. Ilgen, I. Dinçer, M. Yildiz, E. Alptekin, N. Boz, M. Canakci, A.N. Akin, Turk. J. Chem. 31 (2007) 509–514.

[38] M.C.G. Albuquerque, J. Santamaría-González, J.M. Mérida-Robles, R. Moreno-Tost, E. Rodríguez-Castellón, A. Jiménez-López, D.C.S. Azevedo, C.L. Cavalcante, P. Maireles-Torres, Appl. Catal. Gen. 347 (2008) 162–168.

[39] J.L. Shumaker, C. Crofcheck, S.A. Tackett, E. Santillan-Jimenez, T. Morgan, Y. Ji, M. Crocker, T.J. Toops, Appl. Catal., B 82 (2008) 120–130.